Report

Spatial Parkin Translocation and Degradation of Damaged Mitochondria via Mitophagy in Live Cortical Neurons

Qian Cai,[1,2,*] Hesham Mostafa Zakaria,[1,3] Anthony Simone,[1] and Zu-Hang Sheng[1,*]
[1]Synaptic Functions Section, Porter Neuroscience Research Center, National Institute of Neurological Disorders and Stroke, National Institutes of Health, Room 2B-215, 35 Convent Drive, Bethesda, MD 20892-3706, USA
[2]Department of Cell Biology and Neuroscience, Rutgers University, 604 Allison Road, Piscataway, NJ 08854-6999, USA
[3]Howard Hughes Medical Institute, National Institutes of Health Research Scholars Program, 1 Cloister Court, Building 60, Bethesda, MD 20814, USA

Summary

Mitochondria are essential for neuronal survival and function. Proper degradation of aged and damaged mitochondria through mitophagy is a key cellular pathway for mitochondrial quality control. Recent studies have indicated that PINK1/Parkin-mediated pathways ensure mitochondrial integrity and function [1–8]. Translocation of Parkin to damaged mitochondria induces mitophagy in many nonneuronal cell types [9–16]. However, evidence showing Parkin translocation in primary neurons is controversial [9, 15, 17, 18], leaving unanswered questions as to how and where Parkin-mediated mitophagy occurs in neurons. Here, we report the unique process of dissipating mitochondrial $\Delta\psi_m$-induced and Parkin-mediated mitophagy in mature cortical neurons. Compared with nonneuronal cells, neuronal mitophagy is a much slower and compartmentally restricted process, coupled with reduced anterograde mitochondrial transport. Parkin-targeted mitochondria are accumulated in the somatodendritic regions where mature lysosomes are predominantly located. Time-lapse imaging shows dynamic formation and elimination of Parkin- and LC3-ring-like structures surrounding depolarized mitochondria through the autophagy-lysosomal pathway in the soma. Knocking down Parkin in neurons impairs the elimination of dysfunctional mitochondria. Thus, our study provides neuronal evidence for dynamic and spatial Parkin-mediated mitophagy, which will help us understand whether altered mitophagy contributes to pathogenesis of several major neurodegenerative diseases characterized by mitochondrial dysfunction and impaired transport.

Results and Discussion

Mitochondrial Depolarization Induces Slower Parkin Translocation in Mature Neurons

To examine whether mitochondrial depolarization induces Parkin translocation in neurons, we performed three lines of experiments. First, we treated mouse cortical neurons expressing YFP-Parkin and *Discosoma* species red fluorescent protein (dsRed)-Mito at 9–10 days in vitro (DIV) for 24 hr with

*Correspondence: cai@biology.rutgers.edu (Q.C.), shengz@ninds.nih.gov (Z.-H.S.)

vehicle dimethyl sulfoxide (DMSO) as a control, 10 μM carbonyl cyanide *m*-chlorophenyl hydrazone (CCCP; a $\Delta\psi_m$ dissipating reagent), or 10 μM CCCP with lysosomal inhibitors (LIs; 10 μM pepstatin A and 10 μM E64D). Although YFP-Parkin was diffuse in the cytosol of DMSO-treated control neurons (n = 435), it redistributed to mitochondria in 26.67% ± 4.46% of neurons (n = 420) treated with CCCP and in 55.87% ± 6.57% of neurons treated with CCCP/LIs (n = 570) (Figures 1A and 1B). Treatment with CCCP/LIs doubled the percentage of neurons with Parkin translocation relative to CCCP alone (p < 0.001), suggesting that lysosomal degradation capacity has a significant impact on the clearance of Parkin-targeted mitochondria via mitophagy in neurons. Second, we coimmunostained similarly treated neurons with antibodies against neuronal marker MAP2 and mitochondrial markers TOM20 (an outer membrane protein) or cytochrome *c* (a dynamic intermembrane space protein). YFP-Parkin was recruited to mitochondria labeled with TOM20 or cytochrome *c* (Figure 1C) in CCCP-treated neurons, but not in DMSO controls. To examine Parkin translocation kinetics, we imaged neurons at various time points during CCCP treatment. Parkin translocation between 0.5–6 hr was exceptionally rare. Parkin-ring-like structures surrounding fragmented mitochondria were occasionally observed at as early as 12 hr and became increasingly frequent after 18 hr of CCCP treatment (Figure 1D).

To determine whether endogenous Parkin undergoes similar translocation after depolarization, we immunostained cortical neurons at DIV10 with an anti-Parkin antibody following 24 hr CCCP/LIs treatment. Whereas endogenous Parkin appears as a diffuse pattern or as small puncta not colocalized with mitochondria in DMSO-treated neurons, treatment with CCCP/LIs induces endogenous Parkin recruitment to mitochondria (Figure 1E). Alternatively, we isolated the mitochondria-enriched membrane fraction from cultured cortical neurons at DIV13 following the same treatment. Although the majority of Parkin was in the cytosolic fraction, treatment with CCCP/LIs induced endogenous Parkin to associate with the mitochondria-enriched membrane (Figure 1F). Quantitative analysis showed a 2-fold (2.28 ± 0.31) increase in Parkin intensity in the mitochondrial fractions following treatment with CCCP/LIs compared with DMSO (p = 0.0014, n = 3). We also observed elevated levels of the autophagic markers LC3-II and p62/SQSTM1 associated with the mitochondria-enriched membrane fraction. Altogether, these results indicate that mitochondrial depolarization can induce the recruitment of both exogenous and endogenous Parkin in mature neurons.

A gradual but slow increase in Parkin translocation during prolonged CCCP treatment argues against the possibility that CCCP becomes less effective over time in medium. Spiked CCCP media, which had been incubated with neurons for 24 hr, were still effective and sufficient to induce 23.95% ± 2.49% of cultured neurons (fresh) to display Parkin translocation, a percentage close to that when using fresh CCCP (26.67% ± 4.46%) at the same concentration (see Figure S1 available online). These results suggest that Parkin-mediated mitophagy in neurons is a much slower process than in other cell types reported. Treating HeLa cells with 10 μM
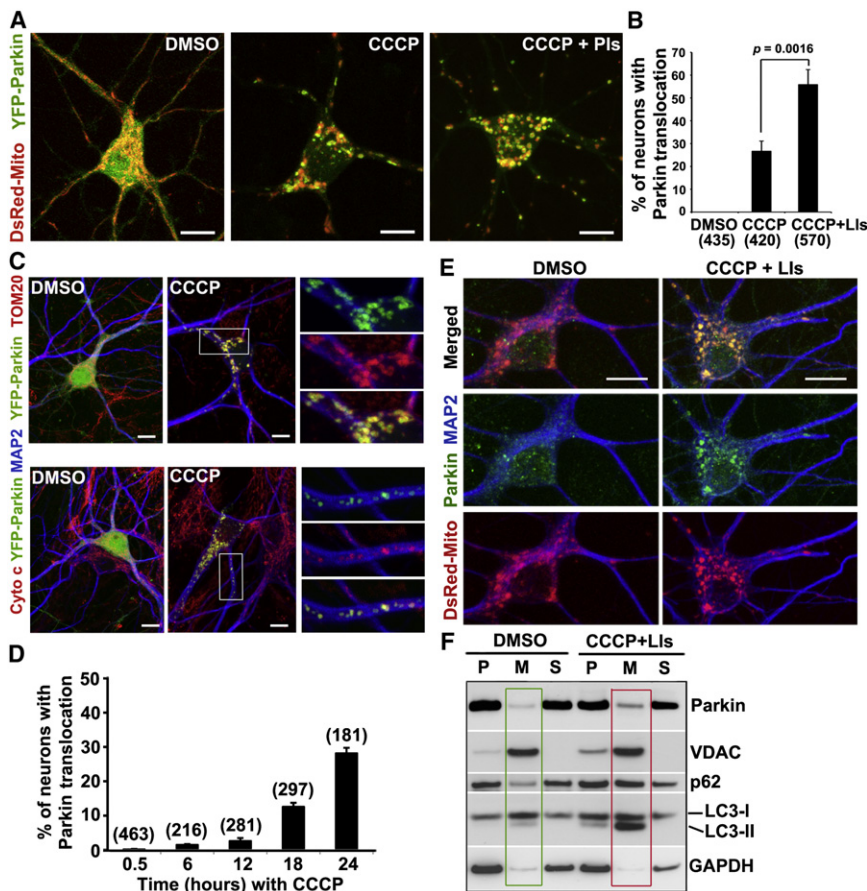
Figure 1. CCCP-Induced Recruitment of Parkin to Mitochondria in Cortical Neurons

(A and B) Representative images (A) and quantitative analysis (B) showing CCCP-induced Parkin translocation to mitochondria. Cortical neurons expressing YFP-Parkin and dsRed-Mito at DIV9 were treated for 24 hr with DMSO, 10 μM CCCP, or 10 μM CCCP + LIs.

(C) CCCP-induced Parkin translocation to mitochondria labeled by mitochondrial marker TOM20 (upper panels) or cytochrome c (lower panels). Cortical neurons expressing YFP-Parkin were treated with DMSO or 10 μM CCCP followed by coimmunostaining with antibodies against MAP2 and TOM20 or cytochrome c. The right three panels show enlarged views of the boxed area.

(D) Time course of Parkin translocation following depolarization. Neurons at DIV8–10 were imaged at sequential time points during CCCP treatment.

(E) Endogenous Parkin translocation to mitochondria. Cortical neurons expressing dsRed-Mito at DIV10 were treated with DMSO or CCCP/LIs for 24 hr, followed by immunostaining with a monoclonal Parkin antibody (Abcam). Note that CCCP/LIs treatment induces the recruitment of endogenous Parkin to mitochondria.

(F) Increased endogenous Parkin associates with mitochondria following CCCP/LIs treatment (red box) relative to that with DMSO control (green box). Cortical neurons at DIV13 were incubated with DMSO or 10 μM CCCP/LIs for 24 hr and then subjected to fractionation into postnuclear supernatant (P), mitochondria-enriched membrane pellet (M), and cytosol supernatant (S). Protein lysates (10 μg) were sequentially immunoblotted with antibodies against Parkin (monoclonal, Santa Crutz) and various markers including voltage-dependent anion channel (mitochondria), glyceraldehyde-3-phosphate dehydrogenase (GAPDH) (cytosol), p62/SQSTM1 and LC3 (autophagy).

Scale bars represent 10 μm. Data was quantified from the number of neurons indicated in parentheses from three or four independent experiments. Error bars represent SEM. Student's t test.

CCCP or SH-SY5Y cells with 20 μM CCCP can induce Parkin association with mitochondria in ∼80% of cells within 1–2 hr [9–11, 17].

Parkin Is Selectively Recruited to Depolarized Mitochondria

To examine whether Parkin-targeted mitochondria display dissipated $\Delta\psi_m$, we pulsed live neurons expressing YFP-Parkin and CFP-Mito with tetramethylrhodamine ethyl ester (TMRE), a $\Delta\psi_m$-dependent dye. Active or healthy mitochondria will accumulate TMRE to have higher TMRE intensity. In DMSO-treated neurons or neurons recovered from CCCP treatment (no Parkin translocation), the majority of CFP-Mito-labeled mitochondria were colabeled by TMRE, reflecting their electrochemically active status (Figure 2A). In contrast, somatic mitochondria with YFP-Parkin translocation displayed reduced or no TMRE staining, suggesting that YFP-Parkin is selectively recruited to depolarized mitochondria (Figures 2A and 2B). We quantified the TMRE mean intensity in somas and normalized to that in DMSO control neurons (Figure 2C). Neurons with Parkin translocation exhibited a 48.3% ± 4.7% (n = 17; p < 0.001) reduction in the TMRE mean intensity relative to recovered neurons (95.9% ± 5.3% n = 16) and DMSO-treated controls (n = 16). Time-lapse TMRE imaging in live cortical neurons demonstrates that acute incubation with 10 μM CCCP during an 11 min recording is sufficient to globally depolarize $\Delta\psi_m$ (Figure S2B). Furthermore, Parkin was gradually recruited to mitochondria in the soma during a 52 min recording time (Figure 2D; Movie S1).

To determine whether endogenous Parkin is critical for eliminating mitochondria with dissipated $\Delta\psi_m$, we suppressed Parkin expression using an RNA interference (RNAi) approach. Cortical neurons were transfected with Parkin small interfering RNA (siRNA) or control siRNA at DIV0 and endogenous Parkin levels were then assessed by immunoblot. Parkin-siRNA specifically and efficiently reduced endogenous Parkin expression to 26.10% ± 7.96% (n = 3) of control levels (Figure 2E). Knocking down Parkin impaired the elimination of dysfunctional mitochondria, leading to accumulation of mitochondria with reduced TMRE intensity (Figures 2F and 2G). After 24 hr CCCP treatment, 66.91% ± 2.00% of control neurons (n = 130) recovered mitochondrial TMRE intensity, versus 19.27% ± 2.01% (n = 97, p < 0.001) of Parkin loss-of-function neurons (Figure 2G). These results support our hypothesis that Parkin-mediated mitophagy is one of the unique neuronal mechanisms to maintain mitochondrial integrity and function in response to dissipating $\Delta\psi_m$. Our RNAi data are consistent with a previous report demonstrating mitochondrial dysfunction and oxidative damage in Parkin-deficient mice [2].

Previous reports noted an absence of Parkin translocation after acute CCCP treatment of primary cortical neurons [15]

Figure 2. Selective Parkin Recruitment to Depolarized Mitochondria

(A–C) Representative images (A and B) and quantitative analysis (C) showing translocation of YFP-Parkin to depolarized mitochondria. Cortical neurons expressing YFP-Parkin and CFP-Mito at DIV9 were treated with DMSO or 10 μM CCCP for 24 hr followed by loading with mitochondrial $\Delta\psi_m$-dependent dye TMRE for 30 min prior to imaging. Arrows indicate depolarized mitochondria labeled by CFP-Mito but unlabeled by TMRE. Arrowheads represent polarized mitochondria marked by both CFP-Mito and TMRE, which are unlabeled by Parkin. TMRE mean intensity was normalized to DMSO control neurons. Note that neurons recovered from CCCP-treatment maintain normal TMRE mean intensity (p < 0.60), whereas neurons displaying Parkin translocation have reduced TMRE mean intensity in the soma (p < 0.001) relative to that of control neurons.

(D) Time-lapse imaging of live cortical neurons showing slow and dynamic recruitment of YFP-Parkin to mitochondria in the soma. Neurons were treated for 24 hr with 10 μM CCCP, followed by 52 min time-lapse imaging. Graphs to the right are line scans of relative dsRed-Mito and YFP-Parkin fluorescence intensities in the images at respective time points (left panels).

(E) siRNA-mediated Parkin knockdown in neurons. Cortical neurons were transfected with Parkin-siRNA or control siRNA at DIV0 and protein was harvested at DIV4. Protein lysates (10 μg) were sequentially immunoblotted with antibodies against Parkin and various markers including HSP60 and Tom20 (mitochondria), p115 (Golgi), GAPDH (cytosol).

(F and G) Representative images (F) and quantitative analysis (G) showing accumulation of depolarized mitochondria by knocking down Parkin in cortical neurons, leading to more mitochondria with reduced or no TMRE staining following CCCP treatment. Arrows point to mitochondria with high TMRE intensity (con small hairpin RNA [shRNA]) or low TMRE intensity (Parkin-shRNA). CFP-Mito*: color is converted from cyan to green for better contrast. Quantitative data was expressed as normalized TMRE mean intensity in the soma (upper graph) or percentage of neurons with recovered TMRE intensity following CCCP treatment (lower graph). Data were collected from the number of neurons indicated in parentheses from three independent experiments. Scale bars in (A) and (F) represent 10 μm and in (B) and (D) represent 5 μm. Error bars represent SEM. Student's t test.

and in dopaminergic neurons with the loss of mitochondrial DNA (mtDNA) [18]. The latter study suggests two different neuronal responses to damaged mitochondria: one for acute $\Delta\psi_m$ dissipation by depolarizing reagents and one for slow progressive deterioration of mitochondrial function by deleting mtDNA in vivo. Thus, Parkin-mediated mitophagy likely serves to ensure neuronal mitochondrial integrity by eliminating severely damaged mitochondria with lost $\Delta\psi_m$ [18]. Our study reveals that neuronal mitophagy is a slower process. In response to 24 hr CCCP treatment, only a small percentage of neurons displayed detectable Parkin translocation, whereas mitochondria in the majority of neurons recover $\Delta\psi_m$. In addition, the efficacy of Parkin-mediated mitophagic flux in neurons is controlled by lysosomal degradation capacity. It is unclear how neurons recover their $\Delta\psi_m$ following prolonged CCCP treatment in culture. Unlike most cells, neurons are wholly dependent upon mitochondrial respiration, thus special mechanisms are required to recover damaged mitochondria after global depolarization. We propose that lysosomal function, proper Parkin expression, slow Parkin translocation, and the elimination of dysfunctional mitochondria are important factors for $\Delta\psi_m$ recovery. In addition, the quality of the neuronal culture is critical to create optimal survival conditions following CCCP treatment; if not met, the uncoupled mitochondria may quickly initiate an apoptotic process before Parkin translocation can be observed. We have established a high neuronal culture quality to meet our live neuron imaging standards with minimal enzymatic, mechanical, chemical, and oxidative damage [19, 20] (see Supplemental Experimental Procedures).

Parkin-Targeted Mitochondria Accumulate in the Somatodendritic Regions

We examined the distribution of Parkin-targeted mitochondria in neurons treated with CCCP/LIs. Translocated YFP-Parkin forms typical ring-like structures surrounding fragmented mitochondria, which predominantly accumulate in the soma and proximal dendritic regions but are hardly detectable in axons and the distal dendritic processes (Figure 3A), suggesting that depolarized mitochondria are selectively accumulated in the somatodendritic regions after prolonged CCCP treatment. Such unique compartmental restriction was consistently observed in neurons treated with a second $\Delta\psi_m$ dissipating reagent antimycin A (1 μM) or the selective ATP synthase inhibitor oligomycin (1 μM) (Figures S2C, S2D, and S3).

This unique distribution pattern suggests that depolarized mitochondria undergo altered transport following prolonged CCCP treatment. To test this possibility, we examined relative mitochondrial mobility following 24 hr CCCP treatment. We selected axons for measuring mitochondrial mobility due to their uniform microtubule organization and polarity. Axonal processes were selected as we previously reported [19, 20] (Supplemental Experimental Procedures). Kymographs were used to quantify relative mobility. In DMSO-treated neurons, 42.7% ± 2.3% (mean ± SEM) of axonal mitochondria are stationary and 57% of mitochondria are mobile, where 35.9% ± 2% undergo anterograde transport and 21.3% ± 2% undergo retrograde transport. In contrast, in neurons with Parkin translocation, anterograde transport was reduced to 13.3% ± 2% (p < 0.001), whereas retrograde transport was relatively increased (36.12% ± 3.67%, p = 0.002), accompanied by reduced velocity and altered flux of axonal mitochondria (Figures 3B–3D). In recovered neurons without Parkin translocation after CCCP treatment, mobility parameters

were similar or slightly changed compared to those in DMSO-treated neurons.

Altered mitochondrial mobility may be protective for neurons under stressful conditions, where healthy mitochondria remain distally, whereas damaged mitochondria return to the soma for degradation. To test this hypothesis, we overexpressed syntaphilin (SNPH), a neuronal mitochondria docking protein that anchors mitochondria to microtubules, to artificially immobilize mitochondria in distal processes [19]. To our surprise, the distribution of Parkin-targeted mitochondria in neurons changed strikingly following CCCP treatment; Parkin was recruited to arrested mitochondria in distal neuronal processes (Figure 3E). This artificial phenotype suggests that once distal mitochondria are immobilized, they will eventually recruit Parkin. Thus, somatodendritic accumulation of Parkin-targeted mitochondria may be coordinately attributed to several factors including (1) reduced anterograde and relatively enhanced retrograde transport leading to more depolarized mitochondria accumulated in the somatodendritic regions during prolonged CCCP treatment and (2) immobilization of mitochondria after slow Parkin translocation, resulting in reduced anterograde flux of damaged mitochondria into distal processes (Figures 3C and 3D). Therefore, a Parkin-mediated process prevents dysfunctional mitochondria from traveling peripherally. Consistently, we observed that Parkin-targeted mitochondria in the soma remain stationary throughout time-lapse recording. This hypothesis is consistent with previous studies showing reduced levels of motor and adaptor proteins upon CCCP-induced mitophagy [12, 13] and a recent report showing that Parkin-dependent degradation of Miro arrests mitochondrial movement [21].

The correlation between $\Delta\psi_m$ and mitochondrial mobility is controversial, especially following acute treatment of neurons with high concentrations of $\Delta\psi_m$ dissipating reagents [22, 23]. In one study with JC-1 staining and acute depolarization with much higher concentrations of antimycin A (100 μM), 90% of mitochondria with high $\Delta\psi_m$ moved in the anterograde direction, whereas 80% with low $\Delta\psi_m$ moved in the retrograde direction [22]. Interestingly, acutely applying a much higher concentration of CCCP (1mM) blocks mitochondrial transport. Another study with TMRM staining showed no correlation between $\Delta\psi_m$ and the direction of axonal mitochondrial transport in sensory neurons [23]. In our study, we instead examined mitochondrial mobility after neuron recovery from 24 hr treatment with a lower concentration of CCCP (10 μM), allowing us to assess the correlation between mobility and slow Parkin translocation. Prolonged $\Delta\psi_m$ dissipation may allow the proceeding slow events to induce mobility changes in neurons, which is supported by our observations that only neurons with Parkin translocation displayed reduced anterograde movement.

Parkin-Targeted Mitochondria Are Eliminated through the Autophagy-Lysosomal Pathway in Somas

To determine whether Parkin-targeted mitochondria are degraded via the autophagy-lysosomal pathway, we labeled autophagic vacuoles with GFP-LC3 [20]. In DMSO-treated conditions, GFP-LC3 was cytosolic (Figure 4A). However, CCCP treatment resulted in LC3-labeled ring-like structures surrounding fragmented mitochondria in the somatodendritic regions. Treating neurons with both CCCP and LIs produced more LC3-labeled mitochondria (yellow) and other autophagic vacuoles (green). These imaging results are consistent with our biochemical observations showing elevated LC3-II and p62
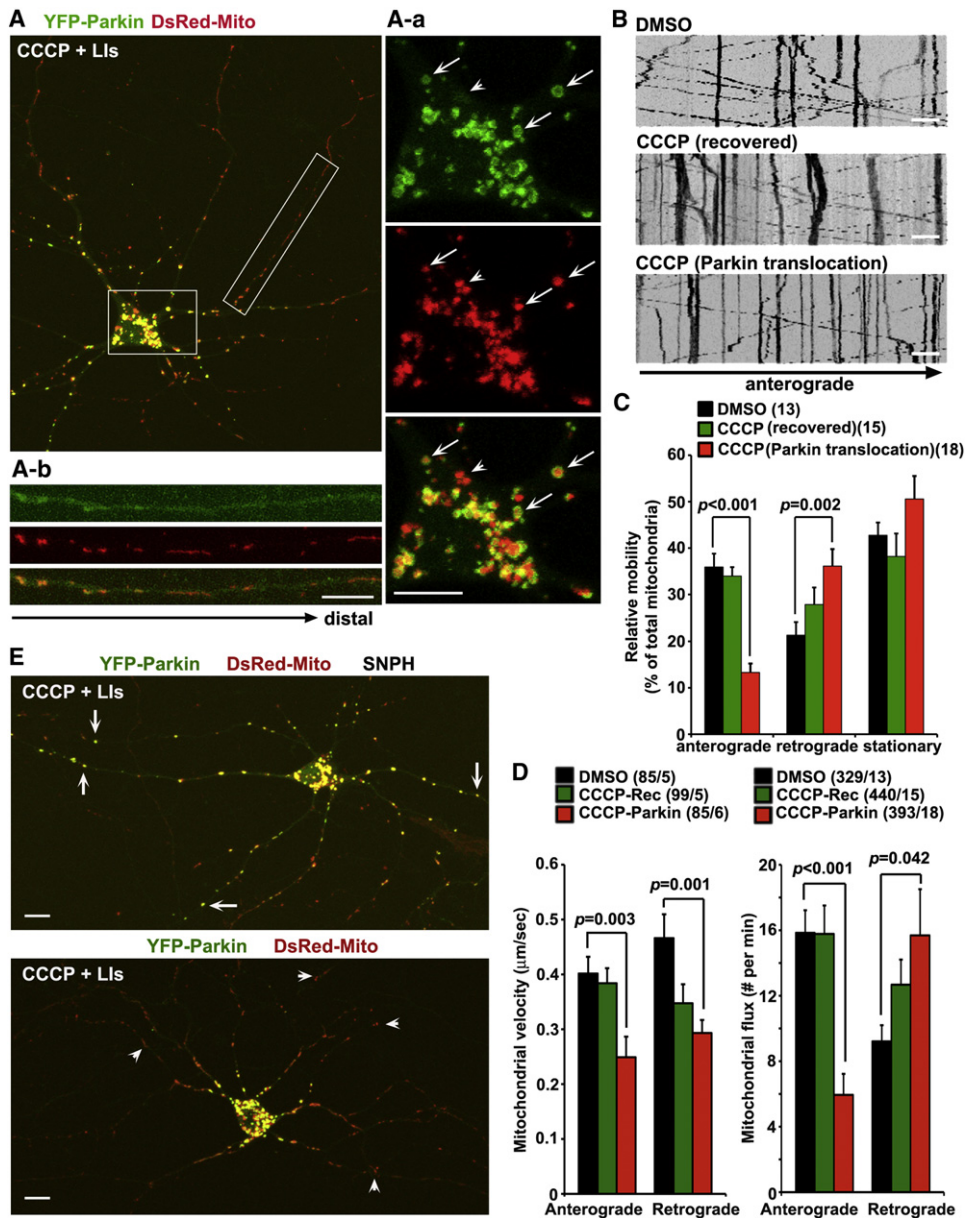
Figure 3. Altered Mitochondrial Transport during Slow Parkin Translocation

(A) Representative images showing CCCP-induced Parkin translocation to mitochondria accumulated in the somatodendritic regions. Cortical neurons at DIV9 were treated for 24 hr with 10 μM CCCP/LIs.

(A-a) Enlarged views of the boxed somatodendritic area. Arrows indicate Parkin ring-like structures surrounding fragmented mitochondria, whereas an arrowhead marks mitochondria unlabeled by Parkin.

(A-b) Enlarged views of a dendritic process showing no Parkin-labeled mitochondria at distal regions.

(B–D) Representative kymographs (B) and quantitative analysis (C and D) showing that Parkin translocation is accompanied by altered mobility, velocity, and flux of axonal mitochondria. Cortical neurons at DIV9 were treated with DMSO or 10 μM CCCP for 24 hr, followed by 15 min time-lapse recordings. Vertical lines represent stationary organelles, oblique lines, or curves to the right represent anterograde transport, and lines to the left indicate retrograde movement. Relative mitochondrial mobility was quantified from the number of neurons (C) or the number of mitochondria and axons (D) indicated in parentheses. Note that neurons recovered from CCCP display normal or slightly altered transport, whereas neurons with Parkin translocation show significant changes in mitochondrial mobility.

(E) Immobilizing mitochondria by expressing SNPH results in Parkin recruitment to distal mitochondria. Cortical neurons coexpressing SNPH (upper panel) or without SNPH overexpression (lower panel) were treated with CCCP/LIs for 24 hr at DIV9. Arrows point to Parkin-targeted distal mitochondria and arrowheads indicate Parkin-negative distal mitochondria in a control neuron.

Error bars represent SEM. Student's t test. Scale bars represent 10 μm.

levels in the mitochondria-enriched fraction following depolarization (Figure 1F). To determine whether depolarized mitochondria were retained within lysosomal organelles upon lysosomal inhibition, we expressed GFP-LAMP1, a lysosomal

membrane protein. In DMSO-treated neurons, there was little colocalization ($2.72\% \pm 0.31\%$) between mitochondria and lysosomes (Figure 4B). In contrast, treatment with CCCP/LIs significantly enhanced the recruitment of mitochondria to
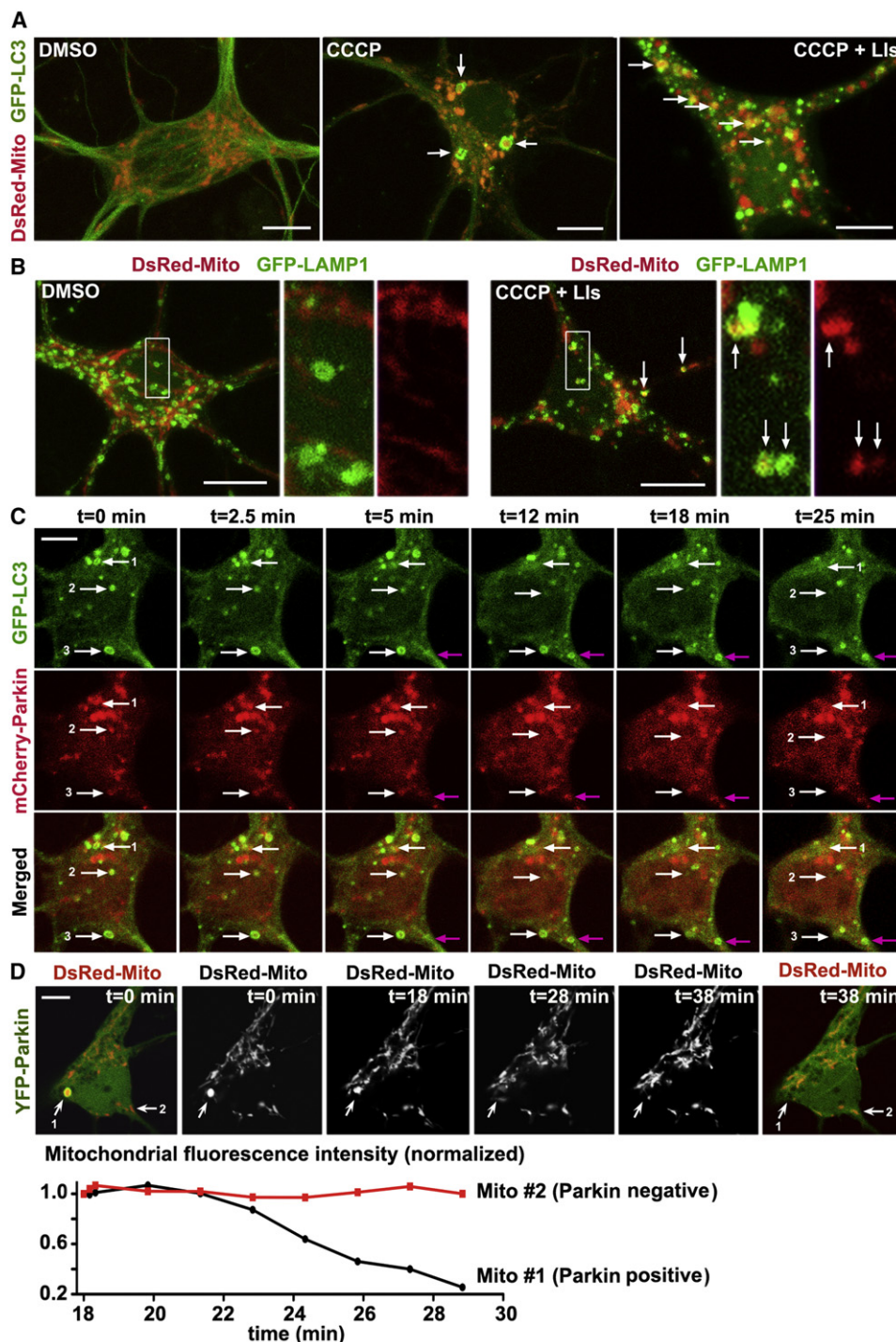
Figure 4. Parkin-Targeted Mitochondria Are Degraded through the Autophagy-Lysosomal Pathway in the Somatodendritic Regions

(A) Representative images showing CCCP-induced LC3 recruitment to depolarized mitochondria. Cortical neurons expressing GFP-LC3 and dsRed-Mito at DIV9 were treated with DMSO, 10 μM CCCP, or 10 μM CCCP/LIs for 24 hr. Arrows indicate colocalization of mitochondria with GFP-LC3.

(B) CCCP-induced colocalization of mitochondria and lysosomes (indicated by arrows). Neurons expressing GFP-LAMP1 and dsRed-Mito at DIV9 were treated with DMSO or 10 μM CCCP/LIs for 24 hr.

(C) Time-lapse imaging showing dynamic emergence and disappearance of Parkin and LC3-labeled autophagic vacuoles in the somatodendritic regions. Neurons expressing GFP-LC3 and mCherry-Parkin were treated for 24 hr with 10 μM CCCP, followed by time-lapse imaging. Whereas colocalized ring-like structures of mCherry-Parkin and GFP-LC3 (white arrows) gradually disappeared, some new puncta (red arrows) emerged during the 25 min recording time.

(D) Time-lapse imaging showing disappearance of a Parkin-associated mitochondrion (#1) in the soma following treatment with 10 μM CCCP. Lower panel shows normalized dsRed-Mito fluorescence intensity of the mitochondrion #1 (Parkin-positive) and #2 (Parkin-negative). Fluorescence intensity for Mito #1 gradually disappears during a 38 min recording period. DsRed-Mito fluorescence intensity of Mito #2 remained consistent throughout the imaging acquisition. Fluorescence intensity of each mitochondrion was normalized to their intensity at t = 18 min. Scale bars in (A) and (B) represent 10 μm and in (C) and (D) represent 5 μm.

LAMP1-labeled lysosomes in the soma (32.10% ± 2.17%, p < 0.001). This indicates that proper lysosomal function is required to efficiently eliminate damaged mitochondria.

We next examined Parkin and LC3-labled mitochondrial dynamics in the somatodendritic regions (Figure 4C). During a 25 min time-lapse recording of the soma, ring-like vesicular structures colabeled with GFP-LC3 and mCherry-Parkin disappeared, whereas new puncta emerged. Furthermore, a ring-like Parkin-associated mitochondrion, as opposed to the Parkin-negative mitochondria in the same image, disappeared over a 38 min time-lapse recording period (Figure 4D; Movie S2). Both the Parkin-ring structure and the mitochondrion were eliminated, whereas the Parkin-unlabeled mitochondrion remained. Thus, our study provides live neuronal evidence showing degradation of Parkin-targeted mitochondria through the autophagy-lysosomal pathway.

Although somatodendritic Parkin-mediated mitophagy is readily and consistently detected in our cultures, it was hardly detectable along distal axonal processes. Alternatively, GFP-LC3 in cortical neurons was recruited to axonal mitochondria following 24 hr treatment with CCCP/LIs (Figure S4). Thus, axonal mitochondria may undergo either Parkin-mediated mitophagy at undetectable Parkin signals or Parkin-independent mitophagy. Further investigation is required to determine the main mechanism for axonal mitochondrial quality control.

Dysfunctional mitochondria not only produce energy less efficiently, but also release harmful reactive oxygen species and initiate apoptotic signaling cascades, all linked to the pathogenesis of major neurodegenerative disorders [24–28]. Sequestration and elimination of aged and damaged mitochondria is an important but poorly characterized neuronal mechanism. In the current study, we reveal several unique features of Parkin-mediated mitophagy in mature cortical neurons. First, Parkin translocation onto mitochondria is slower than in nonneuronal cells. Second, Parkin is selectively recruited to depolarized mitochondria to form ring-like structures. Third, following 24 hr CCCP incubation, Parkin translocation only occurs in a small percentage of neurons. Lysosomal degradation is critical for the efficacy of Parkin-mediated mitophagy. Fourth, Parkin translocation is restricted to the somatodendritic regions, where mature and acidic lysosomes are predominantly localized [20, 29, 30]. This spatial and dynamic process allows neurons to efficiently eliminate dysfunctional mitochondria. Therefore, our study, for the first time, shows selective and dynamic Parkin translocation to depolarized mitochondria and subsequent degradation via the autophagy-lysosomal pathway in live neurons.

Experimental Procedures

Animal care and use were carried out in accordance with National Institutes of Health (NIH) guidelines and approved by the NIH and National Institute of Neurological Disorders and Stroke (NINDS)/National Institute on Deafness and Other Communication Disorders (NIDCD) Animal Care and Use Committee.

Supplemental Information

Supplemental Information includes four figures, Supplemental Experimental Procedures, and two movies and can be found with this article online at doi:10.1016/j.cub.2012.02.005.

Acknowledgments

References

1. Greene, J.C., Whitworth, A.J., Kuo, I., Andrews, L.A., Feany, M.B., and Pallanck, L.J. (2003). Mitochondrial pathology and apoptotic muscle degeneration in Drosophila parkin mutants. Proc. Natl. Acad. Sci. USA 100, 4078–4083.

2. Palacino, J.J., Sagi, D., Goldberg, M.S., Krauss, S., Motz, C., Wacker, M., Klose, J., and Shen, J. (2004). Mitochondrial dysfunction and oxidative damage in parkin-deficient mice. J. Biol. Chem. 279, 18614–18622.

3. Clark, I.E., Dodson, M.W., Jiang, C., Cao, J.H., Huh, J.R., Seol, J.H., Yoo, S.J., Hay, B.A., and Guo, M. (2006). Drosophila pink1 is required for mitochondrial function and interacts genetically with parkin. Nature 441, 1162–1166.

4. Gautier, C.A., Kitada, T., and Shen, J. (2008). Loss of PINK1 causes mitochondrial functional defects and increased sensitivity to oxidative stress. Proc. Natl. Acad. Sci. USA 105, 11364–11369.

5. Deng, H., Dodson, M.W., Huang, H., and Guo, M. (2008). The Parkinson's disease genes pink1 and parkin promote mitochondrial fission and/or inhibit fusion in Drosophila. Proc. Natl. Acad. Sci. USA 105, 14503–14508.

6. Yang, Y., Ouyang, Y., Yang, L., Beal, M.F., McQuibban, A., Vogel, H., and Lu, B. (2008). Pink1 regulates mitochondrial dynamics through interaction with the fission/fusion machinery. Proc. Natl. Acad. Sci. USA 105, 7070–7075.

7. Poole, A.C., Thomas, R.E., Andrews, L.A., McBride, H.M., Whitworth, A.J., and Pallanck, L.J. (2008). The PINK1/Parkin pathway regulates mitochondrial morphology. Proc. Natl. Acad. Sci. USA 105, 1638–1643.

8. Yu, W., Sun, Y., Guo, S., and Lu, B. (2011). The PINK1/Parkin pathway regulates mitochondrial dynamics and function in mammalian hippocampal and dopaminergic neurons. Hum. Mol. Genet. 20, 3227–3240.

9. Narendra, D., Tanaka, A., Suen, D.F., and Youle, R.J. (2008). Parkin is recruited selectively to impaired mitochondria and promotes their autophagy. J. Cell Biol. 183, 795–803.

10. Geisler, S., Holmström, K.M., Skujat, D., Fiesel, F.C., Rothfuss, O.C., Kahle, P.J., and Springer, W. (2010). PINK1/Parkin-mediated mitophagy is dependent on VDAC1 and p62/SQSTM1. Nat. Cell Biol. 12, 119–131.

11. Matsuda, N., Sato, S., Shiba, K., Okatsu, K., Saisho, K., Gautier, C.A., Sou, Y.S., Saiki, S., Kawajiri, S., Sato, F., et al. (2010). PINK1 stabilized by mitochondrial depolarization recruits Parkin to damaged mitochondria and activates latent Parkin for mitophagy. J. Cell Biol. 189, 211–221.

12. Chan, N.C., Salazar, A.M., Pham, A.H., Sweredoski, M.J., Kolawa, N.J., Graham, R.L., Hess, S., and Chan, D.C. (2011). Broad activation of the ubiquitin-proteasome system by Parkin is critical for mitophagy. Hum. Mol. Genet. 20, 1726–1737.

13. Yoshii, S.R., Kishi, C., Ishihara, N., and Mizushima, N. (2011). Parkin mediates proteasome-dependent protein degradation and rupture of the outer mitochondrial membrane. J. Biol. Chem. 286, 19630–19640.

14. Seibler, P., Graziotto, J., Jeong, H., Simunovic, F., Klein, C., and Krainc, D. (2011). Mitochondrial Parkin recruitment is impaired in neurons derived from mutant PINK1 induced pluripotent stem cells. J. Neurosci. 31, 5970–5976.

15. Van Laar, V.S., Arnold, B., Cassady, S.J., Chu, C.T., Burton, E.A., and Berman, S.B. (2011). Bioenergetics of neurons inhibit the translocation response of Parkin following rapid mitochondrial depolarization. Hum. Mol. Genet. 20, 927–940.

16. Van Humbeeck, C., Cornelissen, T., Hofkens, H., Mandemakers, W., Gevaert, K., De Strooper, B., and Vandenberghe, W. (2011). Parkin interacts with Ambra1 to induce mitophagy. J. Neurosci. 31, 10249–10261.

17. Vives-Bauza, C., Zhou, C., Huang, Y., Cui, M., de Vries, R.L., Kim, J., May, J., Tocilescu, M.A., Liu, W., Ko, H.S., et al. (2010). PINK1-dependent recruitment of Parkin to mitochondria in mitophagy. Proc. Natl. Acad. Sci. USA 107, 378–383.

18. Sterky, F.H., Lee, S., Wibom, R., Olson, L., and Larsson, N.G. (2011). Impaired mitochondrial transport and Parkin-independent degeneration of respiratory chain-deficient dopamine neurons in vivo. Proc. Natl. Acad. Sci. USA *108*, 12937–12942.

19. Kang, J.S., Tian, J.H., Pan, P.Y., Zald, P., Li, C., Deng, C., and Sheng, Z.H. (2008). Docking of axonal mitochondria by syntaphilin controls their mobility and affects short-term facilitation. Cell *132*, 137–148.

20. Cai, Q., Lu, L., Tian, J.H., Zhu, Y.B., Qiao, H., and Sheng, Z.H. (2010). Snapin-regulated late endosomal transport is critical for efficient autophagy-lysosomal function in neurons. Neuron *68*, 73–86.

21. Wang, X., Winter, D., Ashrafi, G., Schlehe, J., Wong, Y.L., Selkoe, D., Rice, S., Steen, J., LaVoie, M.J., and Schwarz, T.L. (2011). PINK1 and Parkin target Miro for phosphorylation and degradation to arrest mitochondrial motility. Cell *147*, 893–906.

22. Miller, K.E., and Sheetz, M.P. (2004). Axonal mitochondrial transport and potential are correlated. J. Cell Sci. *117*, 2791–2804.

23. Verburg, J., and Hollenbeck, P.J. (2008). Mitochondrial membrane potential in axons increases with local nerve growth factor or semaphorin signaling. J. Neurosci. *28*, 8306–8315.

24. Chen, H., and Chan, D.C. (2009). Mitochondrial dynamics—fusion, fission, movement, and mitophagy—in neurodegenerative diseases. Hum. Mol. Genet. *18* (R2), R169–R176.

25. Lin, M.T., and Beal, M.F. (2006). Mitochondrial dysfunction and oxidative stress in neurodegenerative diseases. Nature *443*, 787–795.

26. Schon, E.A., and Przedborski, S. (2011). Mitochondria: the next (neurode)generation. Neuron *70*, 1033–1053.

27. Schapira, A.H. (2008). Mitochondria in the aetiology and pathogenesis of Parkinson's disease. Lancet Neurol. *7*, 97–109.

28. Sheng, Z.H., and Cai, Q. (2012). Mitochondrial transport in neurons: impact on synaptic homeostasis and neurodegeneration. Nat. Rev. Neurosci. *13*, 77–93.

29. Overly, C.C., and Hollenbeck, P.J. (1996). Dynamic organization of endocytic pathways in axons of cultured sympathetic neurons. J. Neurosci. *16*, 6056–6064.

30. Lee, S., Sato, Y., and Nixon, R.A. (2011). Lysosomal proteolysis inhibition selectively disrupts axonal transport of degradative organelles and causes an Alzheimer's-like axonal dystrophy. J. Neurosci. *31*, 7817–7830.